I. Introduction

Because the mature technique and economical considering, Si always plays an important role in the electronics industry. But in optical character, III-V compound semiconductor has better performance than Si material. In recently, the improvement of semiconductor technique on the strained semiconductor material is quickly and significantly. Especially, on the development of Si/SiGe material had significant progress in commercial mass production.

In experiment, the spectrum of p-type Si and Ge had been observed from 60′s [1][2] already. The B-doped SiGe/Si quantum well can create terahertz (THz) laser [10] in recent research. But the acceptor states in semiconductor were the critical part in past theoretical work.

Kohn and Schecheru began the topic from 50′s [11]. But until 70′s, Lipari and Baldereschi had significant progress [12] in this subject. They calculated the Lutting-Kohn Hamiltonian [13] by spherical symmetry part and cubic symmetry part. Spherical symmetry part can be decided first. Then use cubic symmetry part for the perturbation to resolve the ground state of the different kinds of acceptor states. In 1992, Buczko and Bassani continue this method to do the complete calculation for Si and Ge acceptor states [14]. But those are for the bulk material only. It can not be extended to the strained SiGe.

In the study of strained SiGe, we should identify the resonant states issue. Fano at 60′s [15] had discussed the interaction of discrete states and continuous states for resonant states. It will be used in my study. The deformation stress on the SiGe/Si material will be discussed in my research too. The theory for both strained and unstrained $Si_{1-x}Ge_x$/Si semiconductor will be proposed in the study.

II. Theory

A new calculation model is claimed in our research. It can apply to acceptor states for strained and unstrained semiconductor. The SiGe/Si material structure is used in our study. $Si_{1-x}Ge_x$ is grown on (100) Si substrate. Because the lattice mismatch of $Si_{1-x}Ge_x$ layer and Si substrate, the stress occurs on the material interface. The stress will be increased with the higher value of x.

The method of calculation acceptor states with the stress had been considered will be introduced in section 2.1. In section 2.2, we will discuss the effective decision method of the wave functions. And make the calculation easier. The estimation of the resonant states will be shown in section 2.3.

2.1 Theory

2.1.1 Calculation of Acceptor States

The most important part for calculation of acceptor states are the choice of wave functions. How to decide the effective wave functions to get the results. We use group theorem to choose it in our works. Then use the variation method for the system Hamiltonian to decide the energy states.

The spin-orbital interaction has the strong effect in our case. We can not neglect the interaction among split of hole band, heavy

hole band, and light hole band. In some other case, the effect for the first conduction band is considered too.

So we use Luttinger-Kohn effective mass theorem and Bir-Pikus stress theorem in our calculation. Effective Bohr radius $a_B^* = \frac{\hbar^2 \varepsilon_0 \gamma_1}{e^2 m}$ is for length unit. And effective Rydberg $Ry^* = \frac{e^4 m}{2\hbar^2 \varepsilon_0^2 \gamma_1}$ is for energy unit.

We use the linear combinations of unstrained Bloch functions at Γ point in reciprocal lattice for the acceptor wave functions:

$$\psi(r) = \sum_{j=1}^{6} F_j(r)\phi_j \qquad (1)$$

$F_j(r)$ are the envelope functions, ϕ_j are the Bloch functions at the band edge of heavy hole band, light hole band, and split of hole band.

$$\text{Heavy hole}: \quad \phi_1 = \frac{1}{\sqrt{2}}(X+iY)\uparrow,\ \phi_4 = \frac{i}{\sqrt{2}}(X-iY)\downarrow$$

$$\text{Light hole}: \quad \phi_2 = \frac{i}{\sqrt{6}}[(X+iY)\downarrow -2Z\uparrow],\ \phi_3 = \frac{1}{\sqrt{6}}[(X-iY)\uparrow +2Z\downarrow]$$

$$\text{Split of hole}: \quad \phi_5 = \frac{1}{\sqrt{3}}[(X+iY)\downarrow +Z\uparrow],\ \phi_6 = \frac{i}{\sqrt{3}}[-(X-iY)\uparrow +Z\downarrow] \qquad (2)$$

Those untrained functions for basis, $F_j(r)$ are the solutions of the effective mass equation [13]:

$$F(r) \equiv \psi(r) = \sum_{j=1}^{6} F_j(r)\phi_j$$

$$\widehat{H}F(r) = EF(r) \qquad (3)$$

Hamiltonian $\widehat{H}$（included stress term）：

$$\widehat{H} = -\begin{bmatrix} P+Q+V & -S & R & 0 & \frac{-1}{\sqrt{2}}S & \sqrt{2}R \\ -S^{\dagger} & P-Q+V & 0 & R & -\sqrt{2}Q & \sqrt{\frac{3}{2}}S \\ R^{\dagger} & 0 & P-Q+V & S & \sqrt{\frac{3}{2}}S^{\dagger} & \sqrt{2}Q \\ 0 & R^{\dagger} & S^{\dagger} & P+Q+V & -\sqrt{2}R^{\dagger} & \frac{-1}{\sqrt{2}}S^{\dagger} \\ \frac{-1}{\sqrt{2}}S^{\dagger} & -\sqrt{2}Q & \sqrt{\frac{3}{2}}S & -\sqrt{2}R & P+\Delta+V & 0 \\ \sqrt{2}R^{\dagger} & \sqrt{\frac{3}{2}}S^{\dagger} & \sqrt{2}Q & \frac{-1}{\sqrt{2}}S & 0 & P+\Delta+V \end{bmatrix} \begin{matrix} \phi_1 \\ \phi_2 \\ \phi_3 \\ \phi_4 \\ \phi_5 \\ \phi_6 \end{matrix}$$

（4）

$P = P_k + P$ ， $Q = Q_k + Q_\varepsilon$ ， $R = R_k + R_\varepsilon$ ， $S = S_k + S_\varepsilon$

$$P_k = (k_x^2 + k_y^2 + k_z^2)$$

$$Q_k = \frac{\gamma_2}{\gamma_1}(k_x^2 + k_y^2 - 2k_z^2)$$

$$R_k = -\frac{\sqrt{3}\gamma_2}{\gamma_1}(k_x^2 - k_y^2) + \frac{i2\sqrt{3}\gamma_3}{\gamma_1}k_x k_x$$

$$S_k = 2\sqrt{3}\frac{\gamma_3}{\gamma_1}(k_x - ik_y)k_z$$

P_ε ， Q_ε ， R_ε ， S_ε are stress term. Because mismatch of the lattice, we can get the value from theorem of Bir-Pikus [16]：

$$P_\varepsilon = -a_v(\varepsilon_{11} + \varepsilon_{22} + \varepsilon_{33})$$

$$Q_\varepsilon = -\frac{b}{2}(\varepsilon_{11} + \varepsilon_{22} - 2\varepsilon_{33})$$

$$R_\varepsilon = \frac{\sqrt{3}}{2}b(\varepsilon_{11} - \varepsilon_{22}) - id\varepsilon_{12}$$

$$S_\varepsilon = -d(\varepsilon_{12} + i\varepsilon_{13})$$

$$\varepsilon_{11} = \varepsilon_{22} = \frac{a_0 - a}{a}$$

$$\varepsilon_{33} = -\frac{C_{12}}{C_{11}}\varepsilon_{11}$$

The lattice constants of $Si_{1-x}Ge_x$ from Ref[17]:

$$a_{Si_{1-x}Ge_x}(x) = a_{Si}(1-x) + a_{Ge}x - 1.88\times10^{-2}\times(x - x^2)(\text{Å})$$

The effect of stress is increase with x. The material parameters are shown in Table 2.1:

Table 2.1 material parameters

	γ_1	γ_2	γ_3	ε_0	Δ	a_v	b	C_{11}	C_{12}	a_0
Si	4.22	0.39	1.44	11.9	44	118.8	−101.45	1.675	1.315	5.43
Ge	13.35	4.25	5.69	15.4	296	59.9	14	0.650	0.494	5.65

It is only the parameters of Si or Ge in the Table 2.1. We use the linear interpolation of Si and Ge to get the parameter of $Si_{1-x}Ge_x$.

2.1.2 Stress Theorem

$Si_{1-x}Ge_x$ grown on Si substrate, the $Si_{1-x}Ge_x$ lattice will have deformation stress. For different direction of the grown axis, the strain reduces the crystal symmetry from T_d to different symmetry.

In (100) case, T_d reduces to D_{2d}. In (110) case, T_d reduces to C_{2v}. In (111) case, T_d reduces to C_{3v}. The different groups have difference to

use the projection operator to choose bases (next section).

Now consider the (100) case first, the crystal symmetry from T_d to D_{2d}. For T_d group, the irreducible representation of the band edge are Γ_8 and Γ_7, the bases are Bloch functions $\{\phi_1, \phi_4\}$, $\{\phi_2, \phi_3\}$ and $\{\phi_5, \phi_6\}$respectively(section 2.2.1). The heavy hole band and the light hole band are degeneracy now; when reduce to the D_{2d} group from the character table:

$$\begin{aligned} \Gamma_8(T_d) &\rightarrow \Gamma_7 + \Gamma_6(D_{2d}) \\ \Gamma_7(T_d) &\rightarrow \Gamma_7(D_{2d}) \end{aligned} \qquad (5)$$

The heavy hole band and the light hole band are split now. The irreducible representation of the band edge are Γ_6 and Γ_7 respectively. The bases of Γ_6 and Γ_7 are $\{\phi_1, \phi_4\}$ and $\{\phi_2, \phi_3\}$, $\{\phi_5, \phi_6\}$. The split of hole band is still Γ_7. With the increase of stress, the tendency of the band edge of split heavy hole band and the light hole band are different. Heavy hole band are upward, but light hole band are downward. The situation is obviously with lager stress. This part will be discussed later.

In equation (4), Hamiltonian can detect the couple only between light hole band and split of hole band with stress:

$$\widehat{H}_{strain} = -\begin{bmatrix} P_\varepsilon + Q_\varepsilon & 0 & 0 & 0 & 0 & 0 \\ 0 & P_\varepsilon - Q_\varepsilon & 0 & 0 & -\sqrt{2}Q_\varepsilon & 0 \\ 0 & 0 & P_\varepsilon - Q_\varepsilon & S & 0 & \sqrt{2}Q_\varepsilon \\ 0 & 0 & 0 & P_\varepsilon + Q_\varepsilon & 0 & 0 \\ 0 & -\sqrt{2}Q_\varepsilon & 0 & 0 & P_\varepsilon + V & 0 \\ 0 & 0 & \sqrt{2}Q_\varepsilon & 0 & 0 & P_\varepsilon + V \end{bmatrix} \begin{matrix} \phi_1 \\ \phi_2 \\ \phi_3 \\ \phi_4 \\ \phi_5 \\ \phi_6 \end{matrix} \qquad (6)$$

In strained case, we can find the ratio of unstrained Bloch functions for each band. From figure 2.1, the coupling of light hole band and split of band can be detected.

If we use the strained Bloch functions in strained case, then we can not detect the coupling of light hole band and split of band.

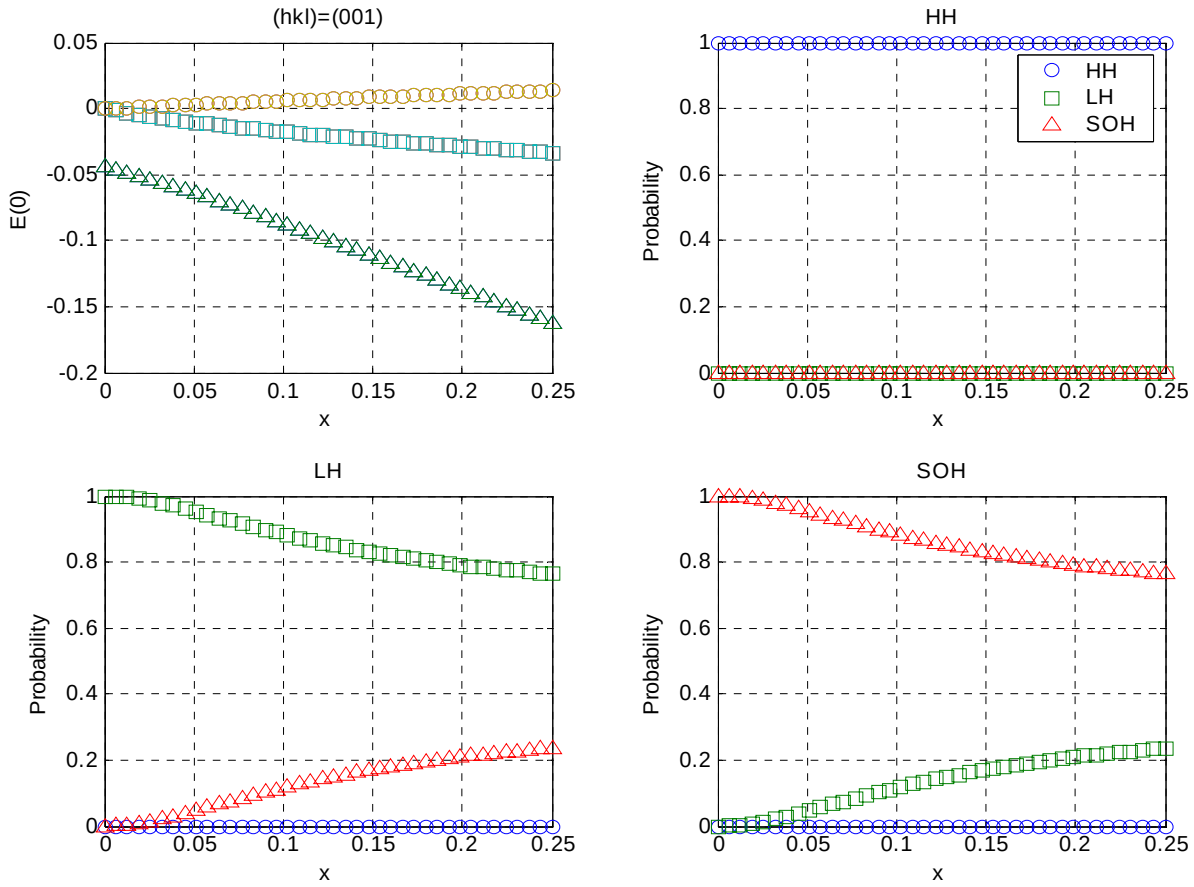

Figure 2.1 The variation of Ge fraction x with different bands

Fig2.1 in left-up, are the variation of Ge fraction x with the band edge,

Fig2.1 in right-up, are the variation of Ge fraction x with the ratio of heavy hole band,

Fig2.1 in left-down, are the variation of Ge fraction x with the ratio of light hole band,

Fig2.1 in right-dowm, are the variation of Ge fraction x with the ratio of split of hole band,

2.2 Wave Functions

2.2.1 Acceptor Wave Functions

In this section, we will discuss how to choose acceptor wave functions and calculate the energy states. Doing the inversion operation P_i for the center of acceptor, the Hamiltonian of effective mass equation is invariable. Envelope functions $F(r)$ and $P_iF(r)$ are the degeneracy eigenfunctions for the same eigenvalue. So we can detect $F(r)$ having odd parity or even parity. Because Bloch functions did not have such kind of character, total acceptor wave functions do not have this character. We use the character of odd parity or even parity to choose the appropriate wave functions.

Consider screening effect and central cell effect from Ref [14], the potential V is:

$$V = \frac{2}{r}[1+(\varepsilon_0 - 1)e^{-\alpha r}] + \frac{A}{r}e^{-\beta r} \qquad (7)$$

The parameter α is from Ref [14]. A and β are semi-experiment parameter to fit the experiment data in Ref [3] ~ [9].

Table 2.2 calculation parameter

A_{Si}	A_{Ge}	α	β
21.9	28.96	0.93	0.96

Envelope functions represent for the linear combination：

$$F_j(r) = \sum_{\substack{l=even \\ \vee odd, m}} f_{l,m}^{(j)}(E,r) Y_l^m \qquad (8)$$

$f_l^j(E,r)$ are radial parts, Y_l^m are spherical harmonics, l are orbital quantum number, m are orbital magnetic quantum number, odd symmetry and even symmetry to $l \le 3$ and $l \le 4$ respectively. For the character of wave function at center of acceptor, radial functions use a set of exponential decrease functions, multiply the polynomial of r [14]：

$$\begin{aligned} f_n^{(l)}(r) &= \sum_k C_k e^{-\alpha_k r} \quad \text{for} \quad l = 0 \\ f_n^{(l)}(r) &= \sum_k C_k r e^{-\alpha_k r} \quad \text{for} \quad l = 1,2,4 \\ f_n^{(l)}(r) &= \sum_k C_k r^2 e^{-\alpha_k r} \quad \text{for} \quad l = 3 \end{aligned} \qquad (9)$$

A set of geometry series is chosen for the parameter α_k：

$$\begin{aligned} \alpha_1 &= 0.01(a.u.) \\ \alpha_k &= 1.5\alpha_1 \end{aligned}$$

Exponential decrease functions can fit bound states localized, and continuous states extending.

Wave functions: (Will discuss on next section and table 2.4)

$$\psi^{\Gamma_6^+}(r)=\begin{pmatrix} f_{00}^1(r)Y_0^0+f_{20}^1(r)Y_2^0+f_{40}^1(r)Y_4^0+f_{44c}^1(r)Y_4^{4c}+f_{44s}^1(r)Y_4^{4s} \\ f_{21}^2(r)Y_2^1+f_{41}^2(r)Y_4^1+f_{4-3}^2(r)Y_4^{-3} \\ f_{22c}^3(r)Y_2^{2c}+f_{22s}^3(r)Y_2^{2s}+f_{42c}^3(r)Y_4^{2c}+f_{42s}^3(r)Y_4^{2s} \\ f_{2-1}^4(r)Y_2^{-1}+f_{4-1}^4(r)Y_4^{-1}+f_{43}^4(r)Y_4^3 \\ f_{21}^5(r)Y_2^1+f_{41}^5(r)Y_4^1+f_{4-3}^5(r)Y_4^{-3} \\ f_{22c}^6(r)Y_2^{2c}+f_{22s}^6(r)Y_2^{2s}+f_{42c}^6(r)Y_4^{2c}+f_{42c}^6(r)Y_4^{2s} \end{pmatrix}^{-1}\begin{pmatrix}\phi_1\\\phi_2\\\phi_3\\\phi_4\\\phi_5\\\phi_6\end{pmatrix} \quad (10a)$$

$$\psi^{\Gamma_6^-}(r)=\begin{pmatrix} f_{32s}^1(r)Y_3^{2s}+f_{32c}^1(r)Y_3^{2c} \\ f_{1-1}^2(r)Y_1^{-1}+f_{33}^2(r)Y_3^3+f_{3-1}^2(r)Y_3^{-1} \\ f_{10}^3(r)Y_1^0+f_{30}^3(r)Y_3^0 \\ f_{11}^4(r)Y_1^1+f_{3-3}^4(r)Y_3^{-3}+f_{31}^4(r)Y_3^1 \\ f_{1-1}^5(r)Y_1^{-1}+f_{33}^5(r)Y_3^3+f_{3-1}^5(r)Y_3^{-1} \\ f_{10}^6(r)Y_1^0+f_{30}^6(r)Y_3^0 \end{pmatrix}^{-1}\begin{pmatrix}\phi_1\\\phi_2\\\phi_3\\\phi_4\\\phi_5\\\phi_6\end{pmatrix} \quad (10b)$$

$$\psi^{\Gamma_7^+}(r)=\begin{pmatrix} f_{2-1}^1(r)Y_2^{-1}+f_{41}^1(r)Y_4^{-1}+f_{43}^1(r)Y_4^3 \\ f_{00}^2(r)Y_0^0+f_{20}^2(r)Y_2^0+f_{40}^2(r)Y_4^0+f_{44c}^2(r)Y_4^{4c}+f_{44s}^2(r)Y_4^{4s} \\ f_{21}^3(r)Y_2^1+f_{41}^3(r)Y_4^1+f_{4-3}^3(r)Y_4^{-3} \\ f_{22c}^4(r)Y_2^{2c}+f_{22s}^4(r)Y_2^{2s}+f_{42c}^4(r)Y_4^{2c}+f_{42s}^4(r)Y_4^{2s} \\ f_{00}^5(r)Y_0^0+f_{20}^5(r)Y_2^0+f_{40}^5(r)Y_4^0+f_{44c}^5(r)Y_4^{4c}+f_{44s}^5(r)Y_4^{4s} \\ f_{21}^6(r)Y_2^1+f_{41}^6(r)Y_4^1+f_{4-3}^6(r)Y_4^{-3} \end{pmatrix}^{-1}\begin{pmatrix}\phi_1\\\phi_2\\\phi_3\\\phi_4\\\phi_5\\\phi_6\end{pmatrix} \quad (10c)$$

$$\psi^{\Gamma_7^-}(r)=\begin{pmatrix} f_{11}^1(r)Y_1^1+f_{3-3}^1(r)Y_3^{-3}+f_{3-1}^1(r)Y_3^1 \\ f_{32s}^2(r)Y_3^{2s}+f_{32c}^2(r)Y_3^{2c} \\ f_{1-1}^3(r)Y_1^{-1}+f_{33}^3(r)Y_3^3+f_{3-1}^3(r)Y_3^{-1} \\ f_{10}^4(r)Y_1^0+f_{30}^4(r)Y_3^0 \\ f_{32s}^5(r)Y_3^{2s}+f_{32c}^5(r)Y_3^{2c} \\ f_{1-1}^6(r)Y_1^{-1}+f_{33}^6(r)Y_3^3+f_{3-1}^6(r)Y_3^{-1} \end{pmatrix}^{-1}\begin{pmatrix}\phi_1\\\phi_2\\\phi_3\\\phi_4\\\phi_5\\\phi_6\end{pmatrix} \quad (10d)$$

The behavior of each energy state can be analysis from those wave functions.

2.2.2 Projection Operator

In each group, each irreducible representation has the corresponding bases functions. For the symmetry operators of this group operating on Bloch functions, we can detect the representation. And check the character to satisfy the corresponding irreducible representation. So we confirm $\{\phi_1, \phi_4\}$ are bases of Γ_6, $\{\phi_2, \phi_3\}$ and $\{\phi_5, \phi_6\}$ are bases of Γ_7:

$$P_O\begin{pmatrix}\phi_1\\ \phi_4\end{pmatrix}=\Gamma_6(O)\begin{pmatrix}\phi_1\\ \phi_4\end{pmatrix},\quad P_O\begin{pmatrix}\phi_2\\ \phi_3\end{pmatrix}=\Gamma_7(O)\begin{pmatrix}\phi_2\\ \phi_3\end{pmatrix},\quad P_O\begin{pmatrix}\phi_5\\ \phi_6\end{pmatrix}=\Gamma_7(O)\begin{pmatrix}\phi_5\\ \phi_6\end{pmatrix} \tag{11}$$

get

$$\Gamma_6(E)=\begin{pmatrix}1&0\\0&1\end{pmatrix}\quad \Gamma_6(C_2^z)=\begin{pmatrix}i&0\\0&-i\end{pmatrix}$$

$$\Gamma_6(C_2^x)=\begin{pmatrix}0&-1\\1&0\end{pmatrix}\quad \Gamma_6(C_2^y)=\begin{pmatrix}0&i\\i&0\end{pmatrix}$$

$$\Gamma_6(\sigma_d)=\begin{pmatrix}0&e^{-i\frac{\pi}{4}}\\-e^{-i\frac{\pi}{4}}&0\end{pmatrix}\quad \Gamma_6(\sigma_d^{'})=\begin{pmatrix}0&-e^{-i\frac{\pi}{4}}\\e^{i\frac{\pi}{4}}&0\end{pmatrix}$$

$$\Gamma_6(S_4)=\begin{pmatrix}e^{i\frac{\pi}{4}}&0\\0&e^{-i\frac{\pi}{4}}\end{pmatrix}\quad \Gamma_6(S_4^{'})=\begin{pmatrix}e^{-i\frac{\pi}{4}}&0\\0&e^{i\frac{\pi}{4}}\end{pmatrix}$$

and

$$\Gamma_7(E)=\begin{pmatrix}1&0\\0&1\end{pmatrix}\quad \Gamma_7(C_2^z)=\begin{pmatrix}-i&0\\0&i\end{pmatrix}$$

$$\Gamma_7(C_2^x)=\begin{pmatrix}0&1\\-1&0\end{pmatrix}\quad \Gamma_7(C_2^y)=\begin{pmatrix}0&i\\i&0\end{pmatrix}$$

$$\Gamma_7(\sigma_d)=\begin{pmatrix}0 & e^{-i\frac{\pi}{4}}\\ -e^{i\frac{\pi}{4}} & 0\end{pmatrix}\qquad \Gamma_6(\sigma_d^{'})=\begin{pmatrix}0 & -e^{i\frac{\pi}{4}}\\ e^{-i\frac{\pi}{4}} & 0\end{pmatrix}$$

$$\Gamma_6(S_4)=\begin{pmatrix}-e^{-i\frac{\pi}{4}} & 0\\ 0 & -e^{i\frac{\pi}{4}}\end{pmatrix}\qquad \Gamma_6(S_4^{'})=\begin{pmatrix}-e^{i\frac{\pi}{4}} & 0\\ 0 & -e^{-i\frac{\pi}{4}}\end{pmatrix}$$

$$\Gamma_i(RO)=-\Gamma_i(O)$$

The trace of the representations conform the character table of D_{2d} group:

Table 2.3 The character table of D_{2d} group

D_{2d}	$1E$	$1R$	C_z, RC_z	(C_x, C_y) $R(C_x, C_y)$	$2S_4$	$2RS_4$	$2\sigma_d, 2R\sigma_d$
Γ_1	1	1	1	1	1	1	1
Γ_2	1	1	1	−1	1	1	−1
Γ_3	1	1	1	1	−1	−1	−1
Γ_4	1	1	1	−1	−1	−1	1
Γ_5	2	2	−2	0	0	0	0
Γ_6	2	−2	0	0	$\sqrt{2}$	$-\sqrt{2}$	0
Γ_7	2	−2	0	0	$-\sqrt{2}$	$\sqrt{2}$	0

The same, all the symmetry operators of this group operating on spherical harmonics, can check the character for satisfy the corresponding irreducible representation, to confirm the bases of Γ_i:

Table 2.4 bases of D_{2d} group

D_{2d}	$l=0$	$l=1$	$l=2$	$l=3$	$l=4$
Γ_1	Y_0^0		Y_2^0	Y_3^{2s}	$Y_4^0;Y_4^{4c}$
Γ_2				Y_3^{2c}	Y_4^{4s}
Γ_3			Y_2^{2c}		Y_4^{2c}
Γ_4		Y_1^0	Y_2^{2s}	Y_3^0	Y_4^{2s}
Γ_5		$\{Y_1^1,Y_1^{-1}\}or\{Y_1^{1c},Y_1^{1s}\}$	$\{Y_2^1,Y_2^{-1}\}or\{Y_2^{1c},Y_2^{1s}\}$	$\{Y_3^3,Y_3^{-3}\}or\{Y_3^{3c},Y_3^{3s}\}$ $\{Y_3^1,Y_3^{-1}\}or\{Y_3^{1c},Y_3^{1s}\}$	$\{Y_4^1,Y_4^{-1}\}$ $\{Y_4^3,Y_4^{-3}\}$

We assume the acceptor wave functions:

$$\psi^{\Gamma_s^i}(r)=\sum_{j=1}^{6}F_j(r)\phi_j=\sum_{j=1}^{6}\sum_{\substack{l=0,2,4\\ \vee l=1,3}}f_l^{\,j}(r)Y_l^m\phi_j \qquad (12)$$

Now $Y_l^m\phi_j$ decide the characteristics of the symmetry. So we use the projection operator from group theorem to decide $Y_l^m\phi_j$ of each symmetry.

The general form of projection operator are：

$$P_{\lambda k}^{(i)}\equiv\frac{l_i}{h}\sum_{P_R}\Gamma^{(i)}(P_R)_{\lambda k}^{*}P_R \qquad (13)$$

l_i are the dimensionality of irreducible representation $\Gamma^{(i)}$, h are the number of symmetry operator P_R, λ and k are the title of column and row.

In D_{2d} group, only two kinds of irreducible representation Γ_6 and Γ_7. Envelope functions $F_j(r)$ have odd parity or even parity. So the wave functions can be decided for Γ_6^+, Γ_7^+, Γ_6^-, Γ_7^- four kinds；Using

projector operator, also can decide the bases corresponding to angular parts:

Table 2.5 envelope functions bases of angular parts

	F_1	F_2	F_3
Γ_6^+	$Y_0^0, Y_2^0, Y_4^0, Y_4^{4c}, Y_4^{4s}$	Y_2^1, Y_4^1, Y_4^{-3}	$Y_2^{2c}, Y_2^{2s}, Y_4^{2c}, Y_4^{2s}$
Γ_7^+	$Y_2^{-1}, Y_4^{-1}, Y_4^3$	$Y_0^0, Y_2^0, Y_4^0, Y_4^{4c}, Y_4^{4s}$	Y_2^1, Y_4^1, Y_4^{-3}
Γ_6^-	Y_3^{2s}, Y_3^{2c}	$Y_1^{-1}, Y_3^3, Y_3^{-1}$	Y_1^0, Y_3^0
Γ_7^-	Y_1^1, Y_3^{-3}, Y_3^1	Y_3^{2s}, Y_3^{2c}	$Y_1^{-1}, Y_3^3, Y_3^{-1}$

	F_4	F_5	F_6
Γ_6^+	$Y_2^{-1}, Y_4^{-1}, Y_4^3$	Y_2^1, Y_4^1, Y_4^{-3}	$Y_2^{2c}, Y_2^{2s}, Y_4^{2c}, Y_4^{2s}$
Γ_7^+	$Y_2^{2c}, Y_2^{2s}, Y_4^{2c}, Y_4^{2s}$	$Y_0^0, Y_2^0, Y_4^0, Y_4^{4c}, Y_4^{4s}$	Y_2^1, Y_4^1, Y_4^{-3}
Γ_6^-	Y_1^1, Y_3^{-3}, Y_3^1	$Y_1^{-1}, Y_3^3, Y_3^{-1}$	Y_1^0, Y_3^0
Γ_7^-	Y_1^0, Y_3^0	Y_3^{2s}, Y_3^{2c}	$Y_1^{-1}, Y_3^3, Y_3^{-1}$

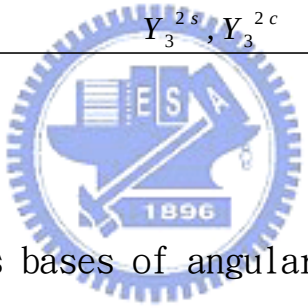

Those envelope functions bases of angular parts are convenient for analysis and prediction of the wave functions.

2.3 Resonant States and Bounded states

The wave functions of the energy states between heavy hole band and light hole band, will couple with the continuum states (here is heavy hole band), and become the resonant states. There are some incorrect continuum states in the calculations. Because we use insufficient numbers of localized bases to describe those are not localized continuum states.

We decide the energy states which belong to heavy hole band, light hole band, or split of hole band. A lot of fake states are contributed by incorrect continuous band, when we increase the number of bases. The energy of those states will be changed. We can not describe the continuous band by the finite bases. Those states are not our interesting.

Decrease α_1 at equation (9) to increase the localized bases. Or increase k at α_k to increase the extending bases. We will get the same result.

Another way is to project the states to the strained band edge. Then decide the states true or false from the ratio of heavy hole band, light hole band, and split of hole band. The transition between strained Bloch functions ϕ_j and unstrained Bloch functions $\tilde{\phi}_j$:

$$\begin{aligned}\phi_j &= \sum_{j'} (M^{-1})_{jj'} \tilde{\phi}_{j'} \\ \tilde{\phi}_j &= \sum_{j'} M_{jj'} \phi_{j'}\end{aligned} \qquad (14)$$

We can represent wave function $\psi(r)$ by unstrained Bloch functions:

$$\begin{aligned}&F_j(r) = \sum_k C_k^{(j)} \varphi_k^{(j)}(r) \\ &\varphi_k^{(j)}(r) = N(L,\alpha_k) r^L e^{-\alpha_k r} Y_l^m(\theta,\phi) \\ &\psi(r) = \sum_j F_j(r)\phi_j = \sum_j \sum_k C_k^{(j)} \varphi_k^{(j)}(r) \sum_{j'} (M^{-1})_{jj'} \tilde{\phi}_{j'} = \sum_{j'} \tilde{F}_{j'}(r) \tilde{\phi}_{j'} \\ &\tilde{F}_{j'}(r) = \sum_j \sum_k C_k^{(j)} (M^{-1})_{jj'} \varphi_k^{(j)}(r)\end{aligned} \qquad (15)$$

The ratio of envelop function $F_j(r)$ at this state are：

$$P_j = \int \left|\tilde{F}_j(r)\right|^2 d^3r = \sum_{j'j''}\sum_{k'k''} C_{k''}^{(j'')} C_{k'}^{(j')} (M^{-1})^*_{j''j} (M^{-1})_{j'j} \left\langle \varphi_{k''}^{(j'')}(r) \middle| \varphi_{k'}^{(j')}(r) \right\rangle \tag{16}$$

P_1+P_4 ， P_2+P_3 ， P_5+P_6 are the ratio of heavy hole band, light hole band, and split of hole band, respectively; The major part of the bounded states above the heavy ole band comes from heavy hole band; The major part of the resonant states between heavy hole band and light hole band comes from light hole band; The major part of the resonant states between light hole band and split of hole band comes from split of hole band. We use them to determine the appropriate states.

III. Result and Discussion

We choose the unstrained band edge of heavy hole band for the zero energy. The degeneracy heavy hole band and light hole band split with the increase of stress. The heavy hole band turns upward with increase of stress. But light hole band and split of hole band turn downward with increase of stress.

The different behaviors of heavy hole band and light hole band can gave the appropriate explanation of the acceptor states variation. It also can be explained by the probability of heavy hole band, light hole band, and split of hole band with the variation of stress.

Figure 3.1 to figure 3.4 are the bounded states variation with stress for different symmetries. All the energy had subtracted the band edge energy already. At the cross section of two states, the wave functions are mixing. In the case of Γ_6^+, the 3rd band and 4th band in figure 3.2, the probability variation with x have the discontinuous at the point which the two energy are degeneracy (figure 3.11 and 3.12). But if we consider the probabilities addition to the two states (figure 3.13). The overall probabilities become continuous. The result implies the discontinuity of the probability for the acceptor states at some x because of mixing of wave functions. So we avoid those areas in figure 3.1 to 3.4.

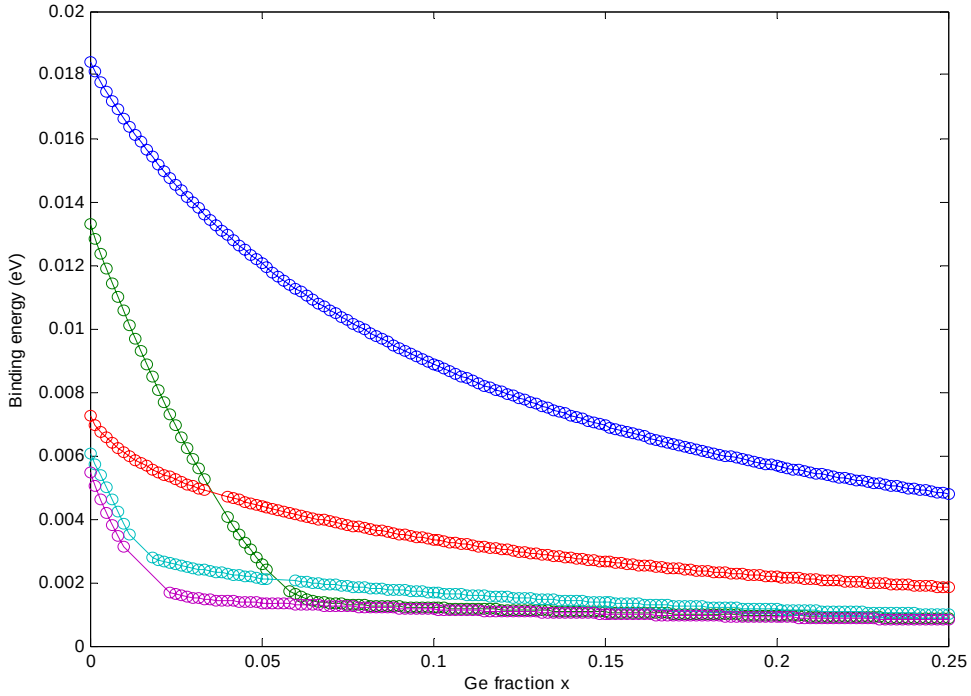

Figure 3.1 $Si_{1-x}Ge_x/Si$(B doped) the bound state of Γ_6^- variation with stress

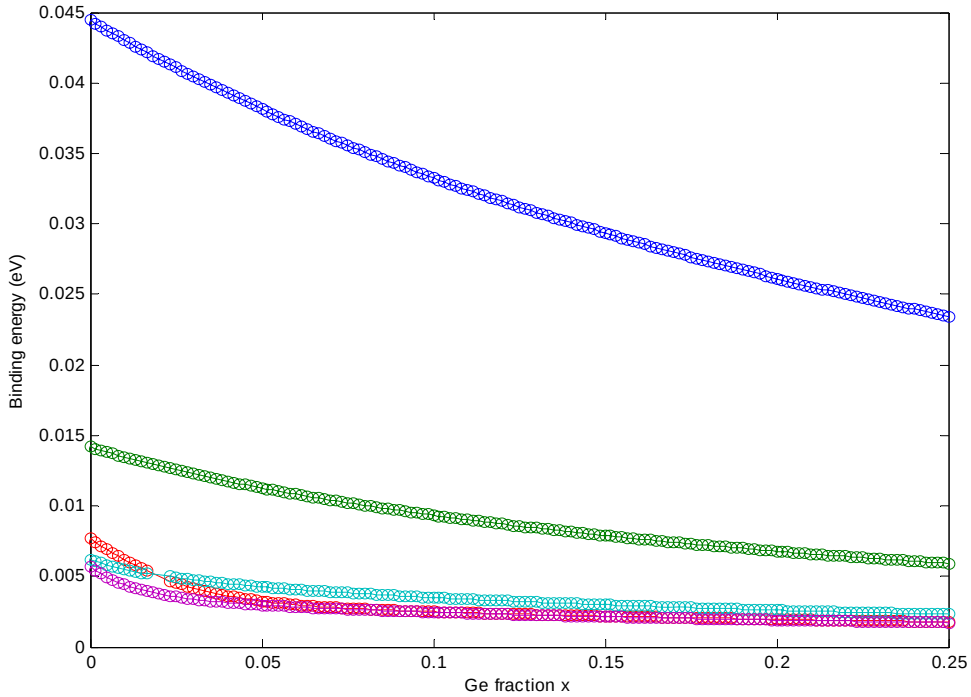

Figure 3.2 $Si_{1-x}Ge_x/Si$(B doped) the bound state of Γ_6^+ variation with stress

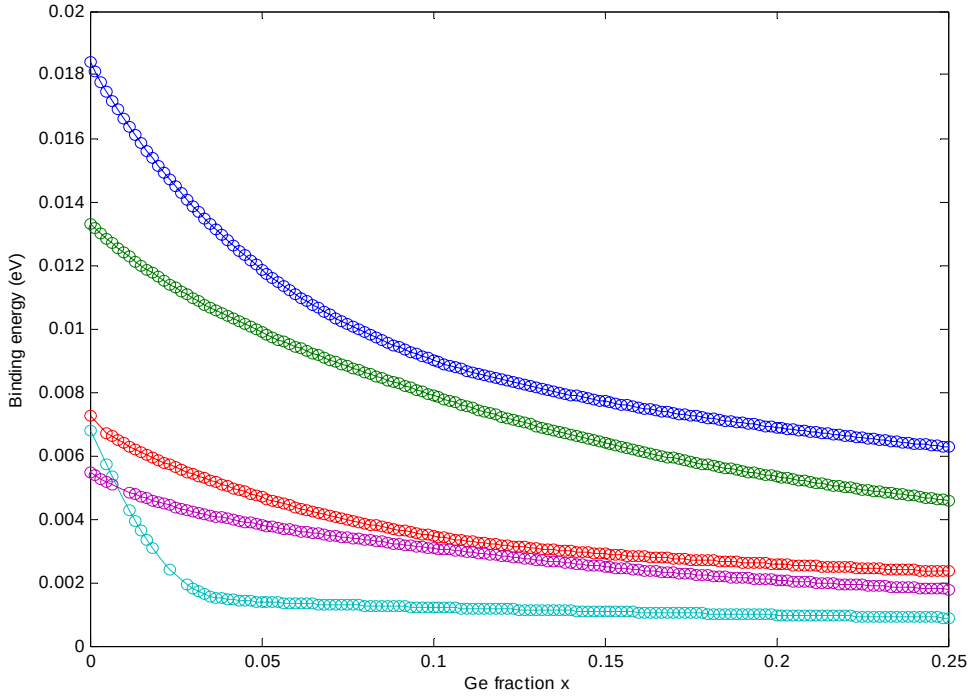

Figure 3.3 $Si_{1-x}Ge_x/Si$(B doped) the bound state of Γ_7^- variation with stress

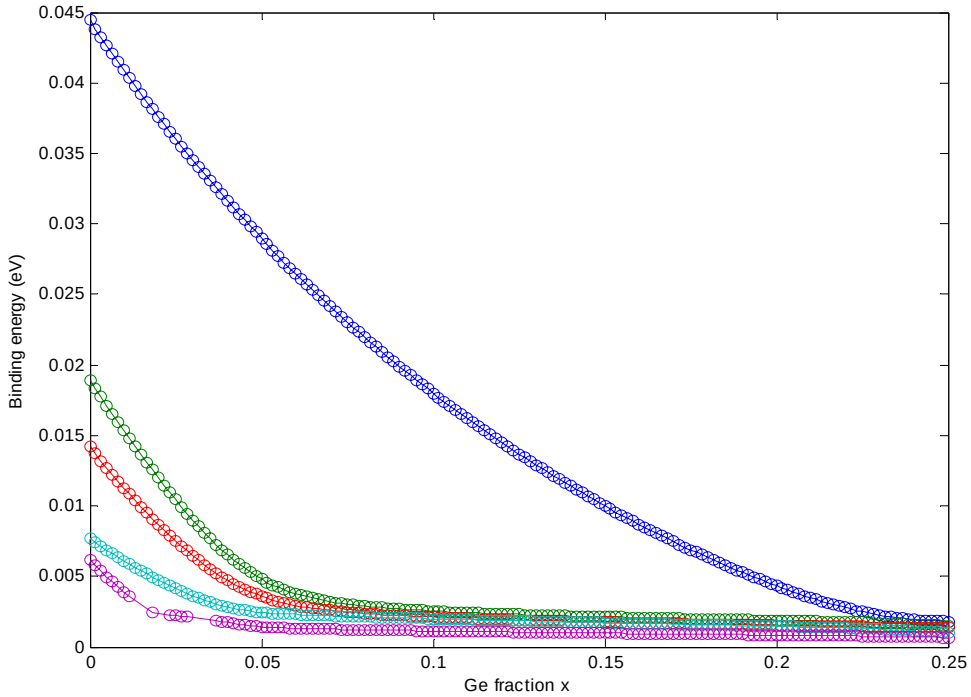

Figure 3.4 $Si_{1-x}Ge_x/Si$(B doped) the bound state of Γ_7^+ variation with stress

3.1 The effect of Stress for Acceptor states

We can analyze the behavior of the lowest 5 states by wave function:

$$\psi^{\Gamma_6^+}(r)=\begin{pmatrix} f_{00}^{1}(r)Y_0^0+f_{20}^{1}(r)Y_2^0+f_{40}^{1}(r)Y_4^0+f_{44c}^{1}(r)Y_4^{4c}+f_{44s}^{1}(r)Y_4^{4s} \\ f_{21}^{2}(r)Y_2^1+f_{41}^{2}(r)Y_4^1+f_{4-3}^{2}(r)Y_4^{-3} \\ f_{22c}^{3}(r)Y_2^{2c}+f_{22s}^{3}(r)Y_2^{2s}+f_{42c}^{3}(r)Y_4^{2c}+f_{42s}^{3}(r)Y_4^{2s} \\ f_{2-1}^{4}(r)Y_2^{-1}+f_{4-1}^{4}(r)Y_4^{-1}+f_{43}^{4}(r)Y_4^{3} \\ f_{21}^{5}(r)Y_2^1+f_{41}^{5}(r)Y_4^1+f_{4-3}^{5}(r)Y_4^{-3} \\ f_{22c}^{6}(r)Y_2^{2c}+f_{22s}^{6}(r)Y_2^{2s}+f_{42c}^{6}(r)Y_4^{2c}+f_{42c}^{6}(r)Y_4^{2s} \end{pmatrix}^{-1}\begin{pmatrix}\phi_1\\ \phi_2\\ \phi_3\\ \phi_4\\ \phi_5\\ \phi_6\end{pmatrix}$$

$$\psi^{\Gamma_6^-}(r)=\begin{pmatrix} f_{32s}^{1}(r)Y_3^{2s}+f_{32c}^{1}(r)Y_3^{2c} \\ f_{1-1}^{2}(r)Y_1^{-1}+f_{33}^{2}(r)Y_3^{3}+f_{3-1}^{2}(r)Y_3^{-1} \\ f_{10}^{3}(r)Y_1^0+f_{30}^{3}(r)Y_3^0 \\ f_{11}^{4}(r)Y_1^1+f_{3-3}^{4}(r)Y_3^{-3}+f_{31}^{4}(r)Y_3^1 \\ f_{1-1}^{5}(r)Y_1^{-1}+f_{33}^{5}(r)Y_3^{3}+f_{3-1}^{5}(r)Y_3^{-1} \\ f_{10}^{6}(r)Y_1^0+f_{30}^{6}(r)Y_3^0 \end{pmatrix}^{-1}\begin{pmatrix}\phi_1\\ \phi_2\\ \phi_3\\ \phi_4\\ \phi_5\\ \phi_6\end{pmatrix}$$

$$\psi^{\Gamma_7^+}(r)=\begin{pmatrix} f_{2-1}^{1}(r)Y_2^{-1}+f_{41}^{1}(r)Y_4^{-1}+f_{43}^{1}(r)Y_4^{3} \\ f_{00}^{2}(r)Y_0^0+f_{20}^{2}(r)Y_2^0+f_{40}^{2}(r)Y_4^0+f_{44c}^{2}(r)Y_4^{4c}+f_{44s}^{2}(r)Y_4^{4s} \\ f_{21}^{3}(r)Y_2^1+f_{41}^{3}(r)Y_4^1+f_{4-3}^{3}(r)Y_4^{-3} \\ f_{22c}^{4}(r)Y_2^{2c}+f_{22s}^{4}(r)Y_2^{2s}+f_{42c}^{4}(r)Y_4^{2c}+f_{42s}^{4}(r)Y_4^{2s} \\ f_{00}^{5}(r)Y_0^0+f_{20}^{5}(r)Y_2^0+f_{40}^{5}(r)Y_4^0+f_{44c}^{5}(r)Y_4^{4c}+f_{44s}^{5}(r)Y_4^{4s} \\ f_{21}^{6}(r)Y_2^1+f_{41}^{6}(r)Y_4^1+f_{4-3}^{6}(r)Y_4^{-3} \end{pmatrix}^{-1}\begin{pmatrix}\phi_1\\ \phi_2\\ \phi_3\\ \phi_4\\ \phi_5\\ \phi_6\end{pmatrix}$$

$$\psi^{\Gamma_7^-}(r)=\begin{pmatrix} f_{11}^{1}(r)Y_1^1+f_{3-3}^{1}(r)Y_3^{-3}+f_{3-1}^{1}(r)Y_3^1 \\ f_{32s}^{2}(r)Y_3^{2s}+f_{32c}^{2}(r)Y_3^{2c} \\ f_{1-1}^{3}(r)Y_1^{-1}+f_{33}^{3}(r)Y_3^{3}+f_{3-1}^{3}(r)Y_3^{-1} \\ f_{10}^{4}(r)Y_1^0+f_{30}^{4}(r)Y_3^0 \\ f_{32s}^{5}(r)Y_3^{2s}+f_{32c}^{5}(r)Y_3^{2c} \\ f_{1-1}^{6}(r)Y_1^{-1}+f_{33}^{6}(r)Y_3^{3}+f_{3-1}^{6}(r)Y_3^{-1} \end{pmatrix}^{-1}\begin{pmatrix}\phi_1\\ \phi_2\\ \phi_3\\ \phi_4\\ \phi_5\\ \phi_6\end{pmatrix}$$

The decrease rate of the even envelop functions Γ_7^+ are faster than Γ_6^+. Because the major contribution of Γ_7^+ from $f_4(r)Y_0^0$ of F_2 and $f_{16}(r)Y_0^0$ of F_5, F_2 and F_5 belong light hole band and split of hole band

respectively. Both of them are decrease with the increase of stress. The major contribution of Γ_6^+ from $f_1(r)Y_0^0$ of F_1, belong heavy hole band, which increase with the increase of stress. So the decrease rate are not so quickly as Γ_7^+.

The same reason also can explain the Γ_6^+ above and Γ_7^+ below after split of $\Gamma_8^+(T_d) \rightarrow \Gamma_7^+ + \Gamma_6^+(D_{2d})$.

The behavior of $\Gamma_8^-(T_d) \rightarrow \Gamma_7^- + \Gamma_6^-(D_{2d})$ are not so obviously like $\Gamma_8^+(T_d) \rightarrow \Gamma_7^+ + \Gamma_6^+(D_{2d})$ by component of wave functions. But still can determine by the probability of $F_1 \sim F_6$ from wave functions. For example, at the case x=0, the ground state of Γ_7^- and Γ_6^-, the probability of $F_1 \sim F_6$ for Γ_7^- ground state are:

F_1=0.170672, F_4=0.318832,

F_2=0.00576199, F_3=0.479972,

F_5=0.015684, F_6=0.00907821

The probability of heavy hole band and light hole band both are 48%. The probability of $F_1 \sim F_6$ for Γ_6^- ground state are：

F_1=0.00554602, F_4=0.480188,

F_2=0.16946, F_3=0.320044,

F_5=0.023938, F_6=0.000824151

Both the probability of heavy hole band and light hole band are 48% too. When x increase, from figure 3.7 and figure 3.9, the ratio of the wave function is still similar. So the variation is almost the same at beginning in figure 3.6. The probability of Γ_7^- and Γ_6^- become different when x between 0.1 and 0.15. Then the Γ_8^- ground state split in this region at figure 3.6. Comparing with figure 3.8 and figure

3.10, we can detect the large difference of Γ_7^+ and Γ_6^+. But Γ_7^- and Γ_6^- are similar. Those can explain the different behaviors for the split of Γ_8^+ and Γ_8^-. If the ratio of light hole band and split of hole band are majority. The decrease rate is faster with increase of stress. On the contrary, if the heavy hole band are majority. The decrease rate is slower with increase of stress.

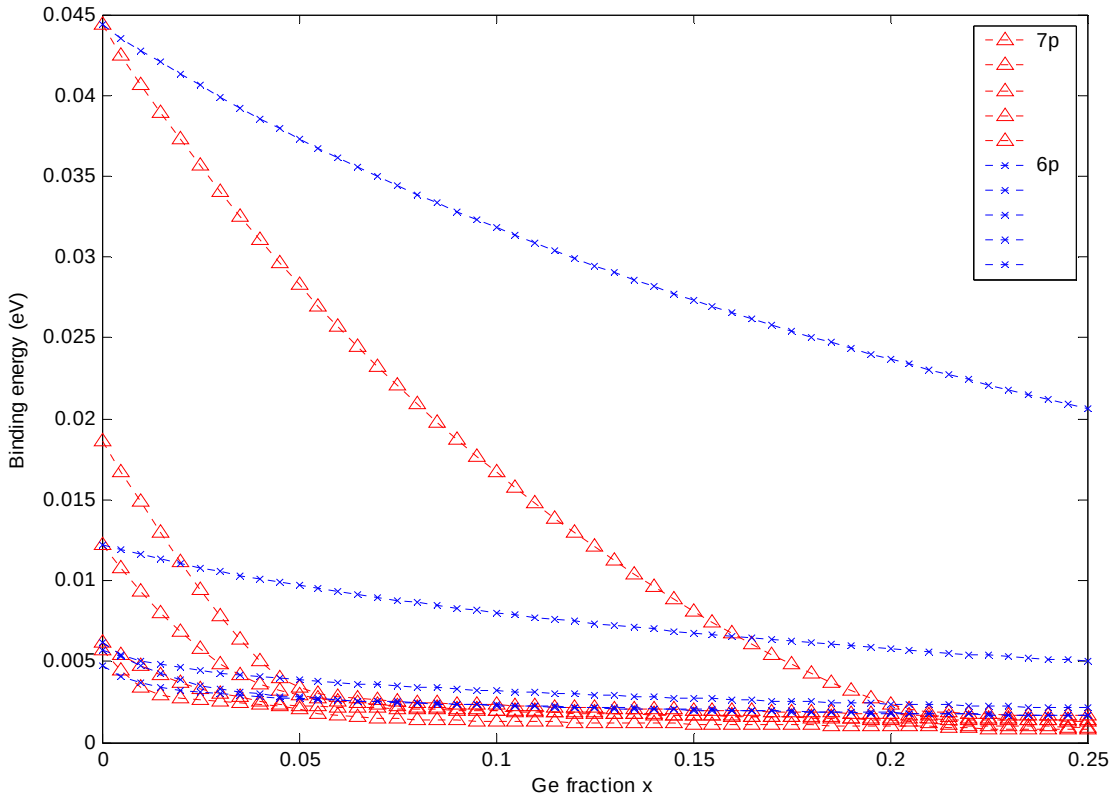

Figure3.5 Γ_8^+ split with x in $Si_{1-x}Ge_x$

We can obviously detect the decrease rate of Γ_7^+ are faster than Γ_6^+. The reason can be explained by the component of wave functions.

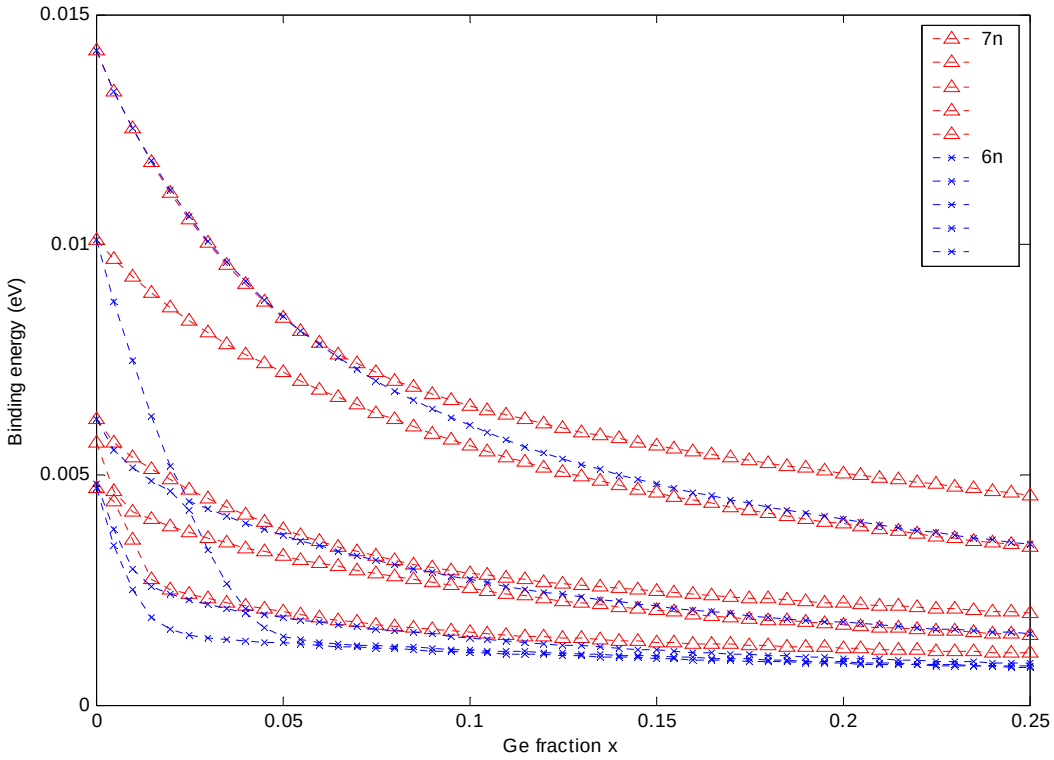

Figure3.6 Γ_8^- split with x in $Si_{1-x}Ge_x$

The decrease rate of Γ_7^- and Γ_6^- can be explained by the ratio of heavy hole band, light hole band, and split of hole band.

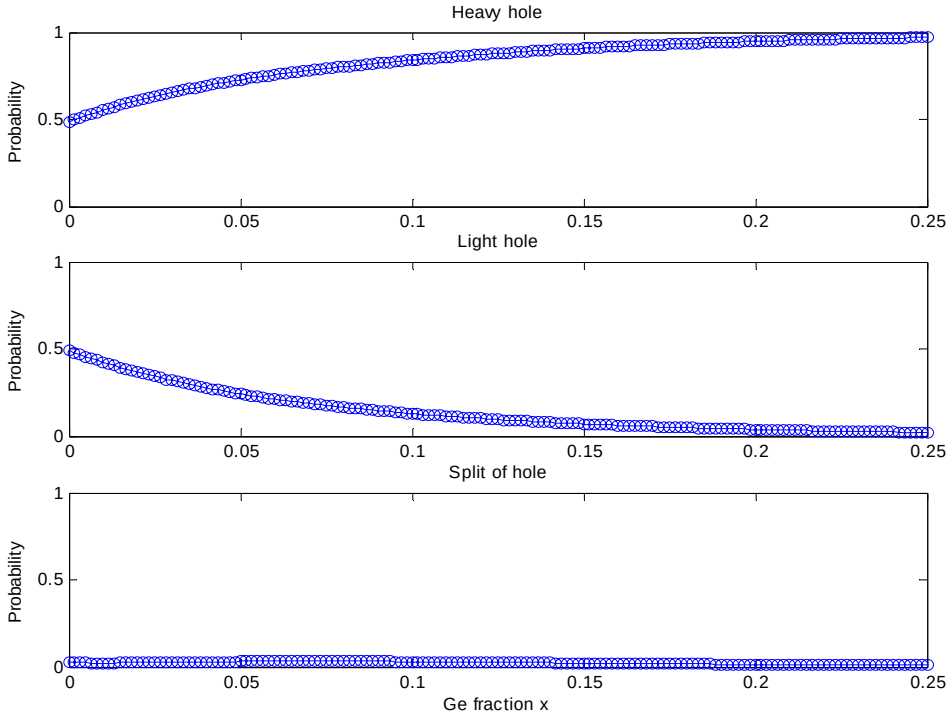

Figure3.7 the probability of HH, LH, and SOH for ground state of Γ_6^- variation with x

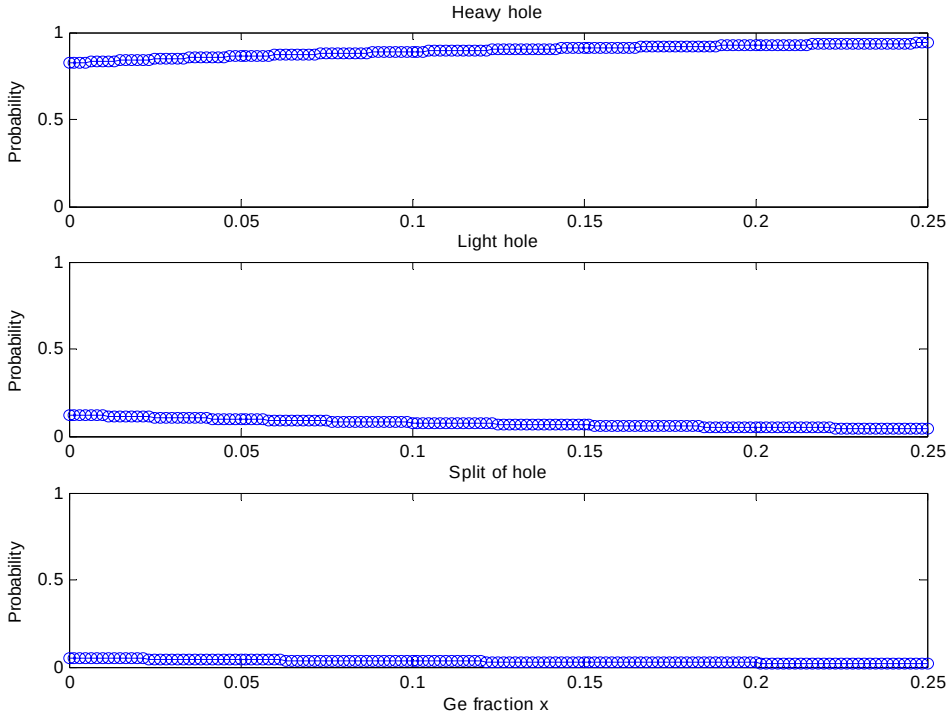

Figure3.8 the probability of HH, LH, and SOH for ground state of Γ_6^+ variation with x

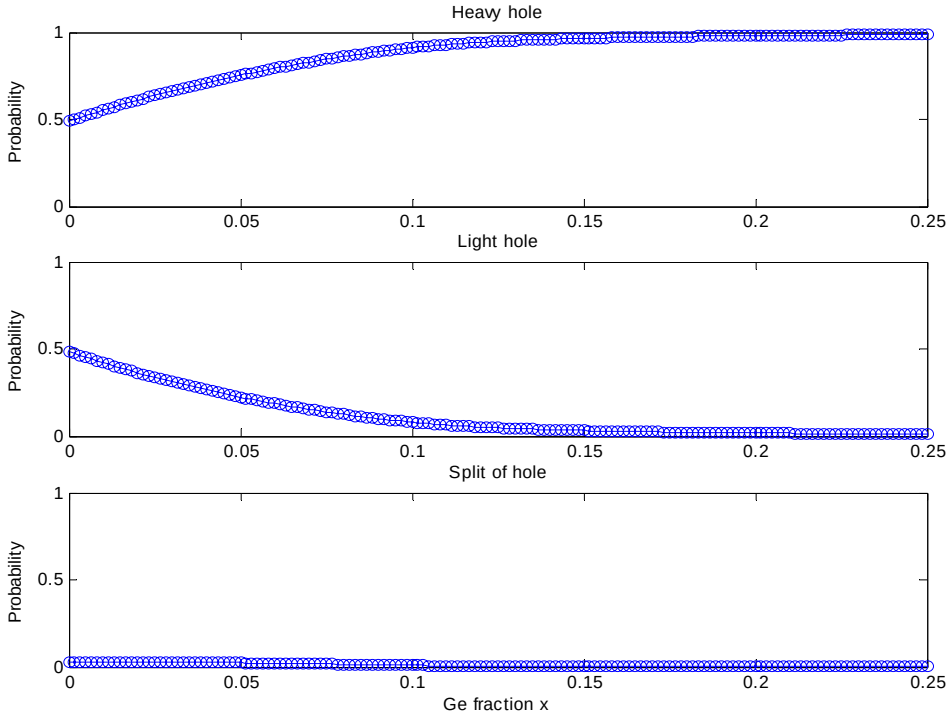

Figure3.9 the probability of HH, LH, and SOH for ground state of Γ_7^- variation with x

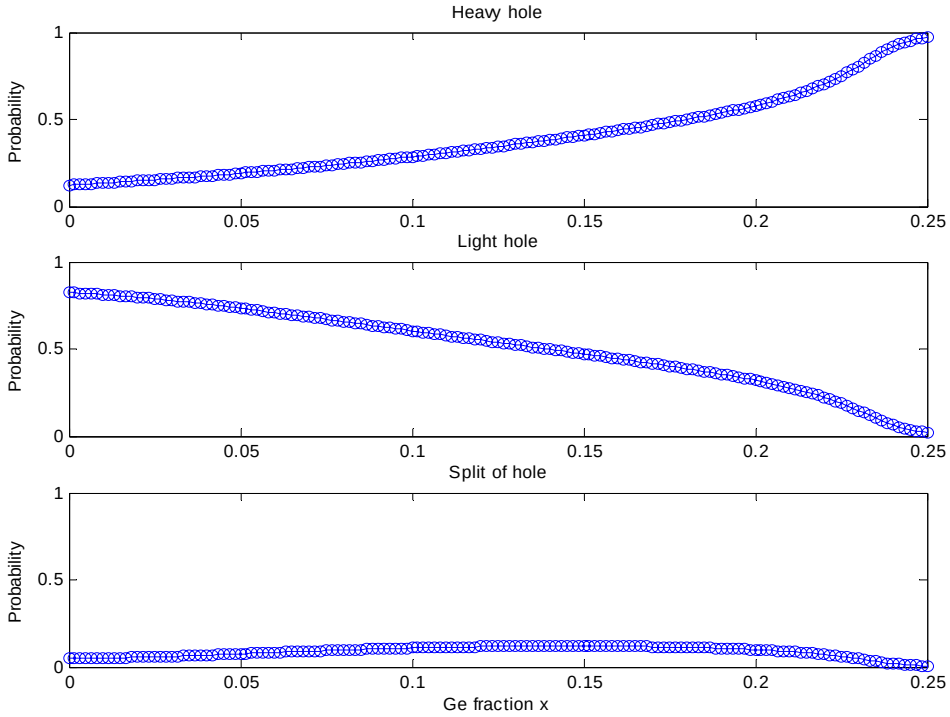

Figure3.10 the probability of HH, LH, and SOH for ground state of Γ_7^+ variation with x

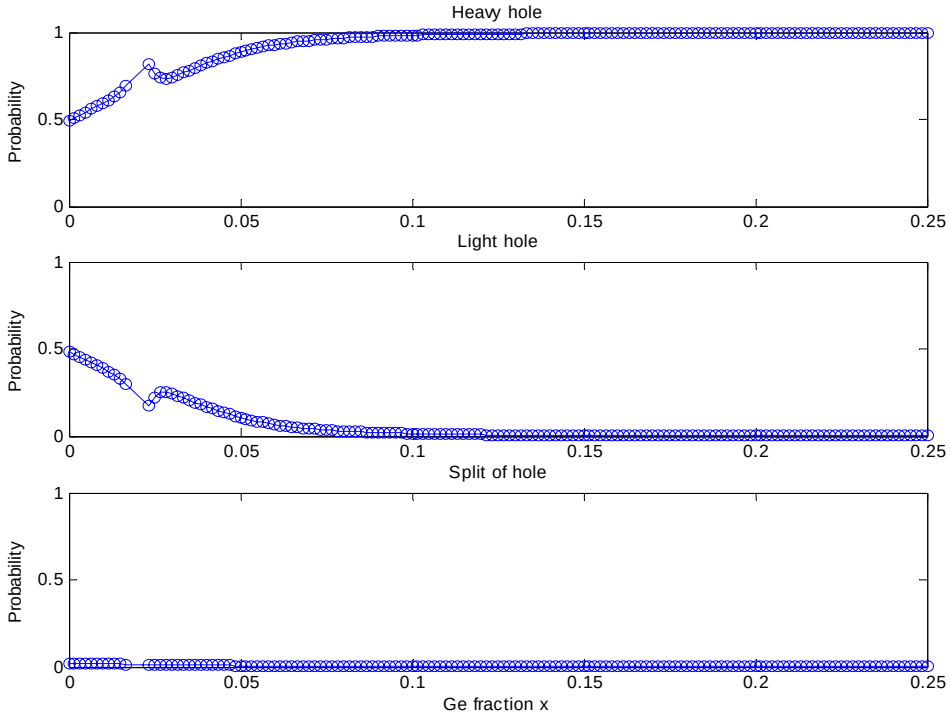

Firure3.11 the probability of HH, LH, and SOH for 2nd excited state of Γ_6^+ variation with x

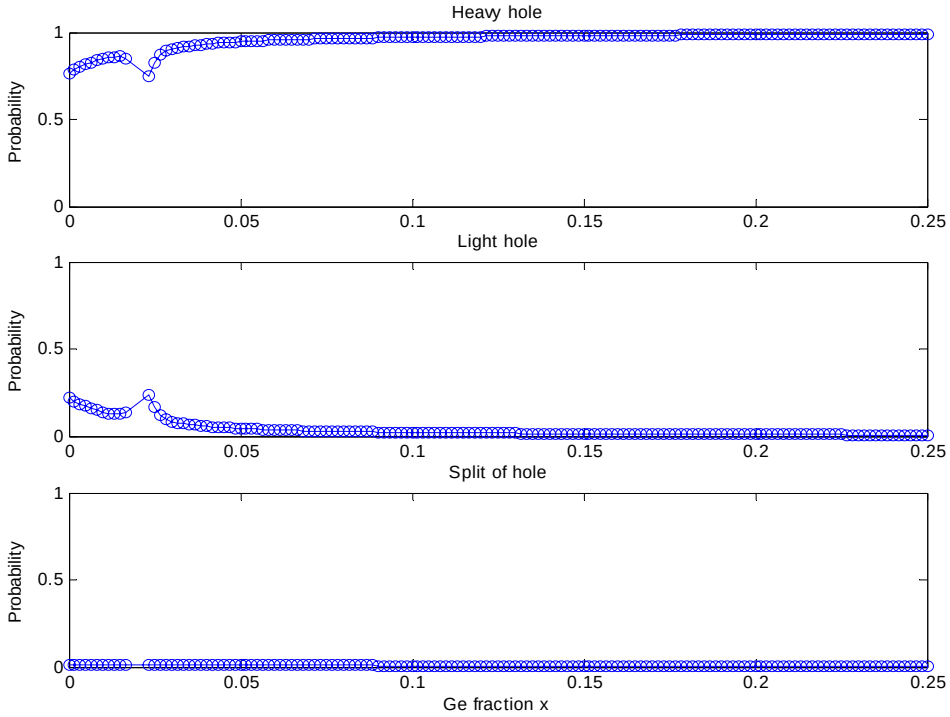

Firure3.12 the probability of HH, LH, and SOH for 3rd excited state of Γ_6^+ variation with x

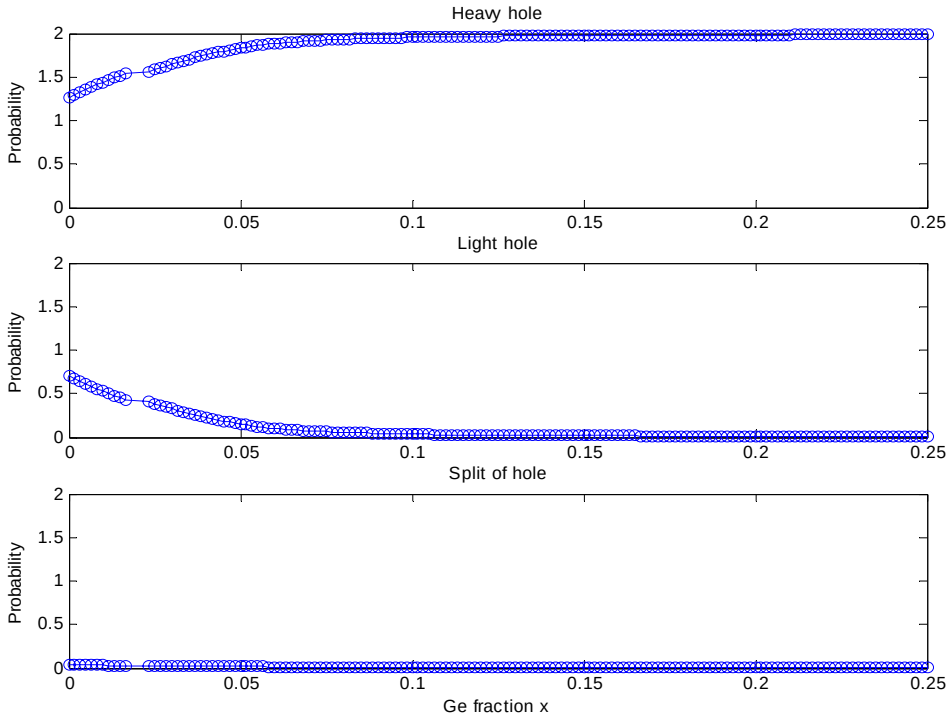

Figure3.13 the probability of HH, LH, and SOH for 2nd excited state of Γ_6^+ plus the probability of HH, LH, and SOH for 3rd excited state of Γ_6^+ variation with x. Because the addition of probability. The vertical axis unit is 2.

3.2 Determine the Resonant states and Bounded States

We can detect the energy states above the degeneracy heavy hole band and light hole band at unstrained case. With the stress not equal to zero, some of the them are moving with heavy hole band. And others are moving with light hole band.

When x from zero to a small value, the symmetry group reduce from T_d to D_{2d} (in 100 direction). The states which moving with heavy hole band or light hole band are already decided. Because the Γ_8 at unstrained case are the degeneracy of Γ_6 and Γ_7. The states belong to Γ_6 will moving with light hole band. And the states belong to Γ_7 will moving with heavy hole band.

From figure 3.15, the states near ground state are belong to Γ_7, which moving with heavy hole band when stress is considered. The states in figure 3.16 are the higher energy states of Γ_8^+ at x=0.

In Figure 3.14, all the states will approach the band edge belong by themselves. This behavior can be observed from figure 3.7 to figure 3.12. The heavy hole band probability of states above heavy hole band will increase with x increasing. At x=0.25, the probability of heavy hole band is almost hundred percent. So the states are very close to the heavy hole band.

The energy of those states is almost the same for increase the number of bases. If the increasing bases are localized bases, the increasing states are all the fake states. If increase the extending bases, the increasing states are higher energy level states. But in those range, they already become continuous states. But the states which we are interesting at lower energy are the same for both kinds of bases increasing.

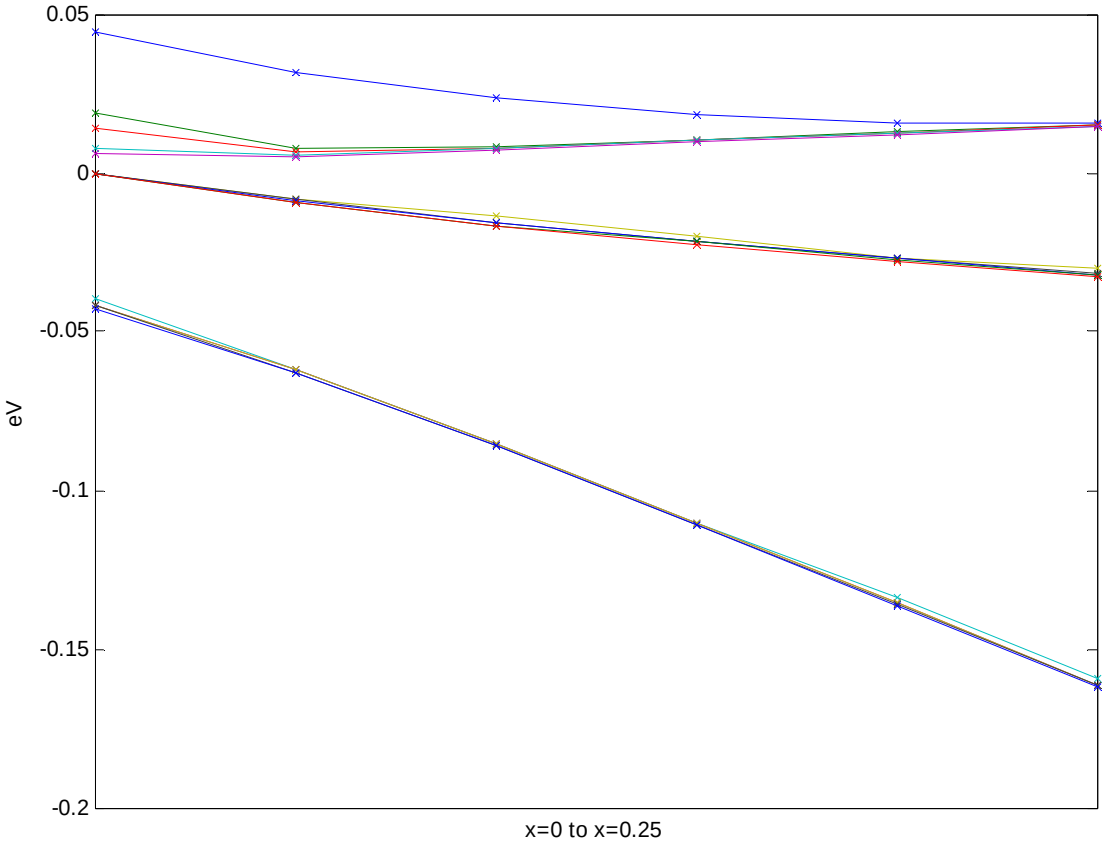

Figure3.14 heavy hole band, light hole band, and split of band, from ground state to 4th excited state, x=0, x=0.05, x=0.1, x=0.15, x=0.2, x=0.25 totally 6 points; all the states will approach the band edge belong by themselves. Figure3.15 to 3.17 are enlargement of heavy hole band, light hole band, and split of band subtract band edge energy respectively.

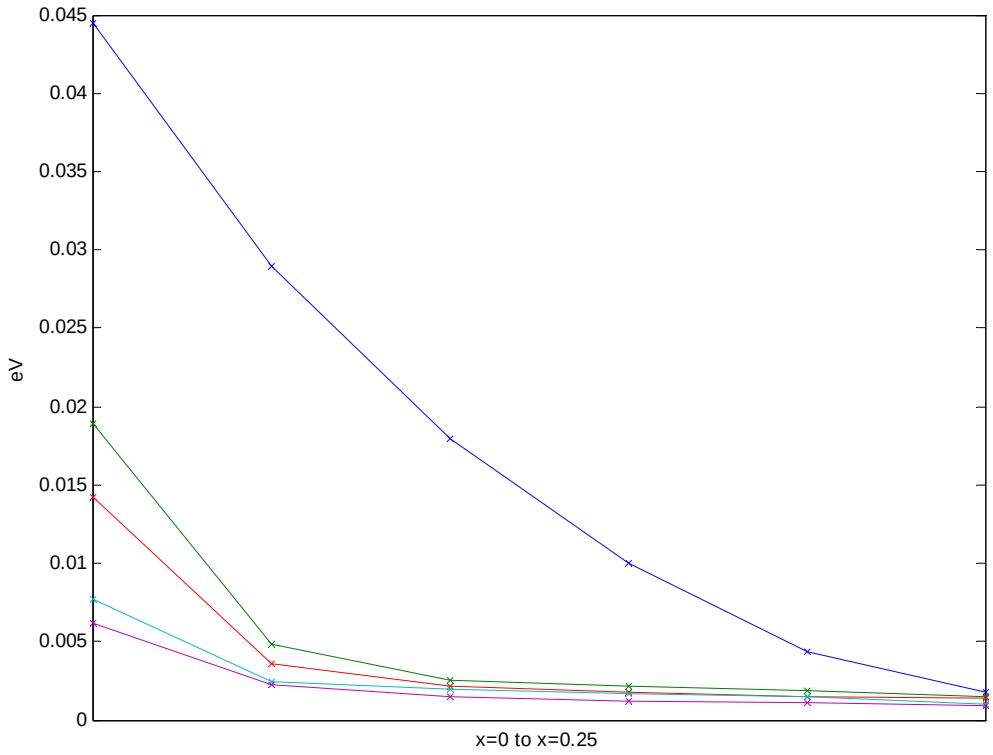

Figure3.15 the bound state energy subtract band edge energy for heavy hole band from ground state to 4th excited state, x=0, x=0.05, x=0.1, x=0.15, x=0.2, x=0.25 totally 6 points.

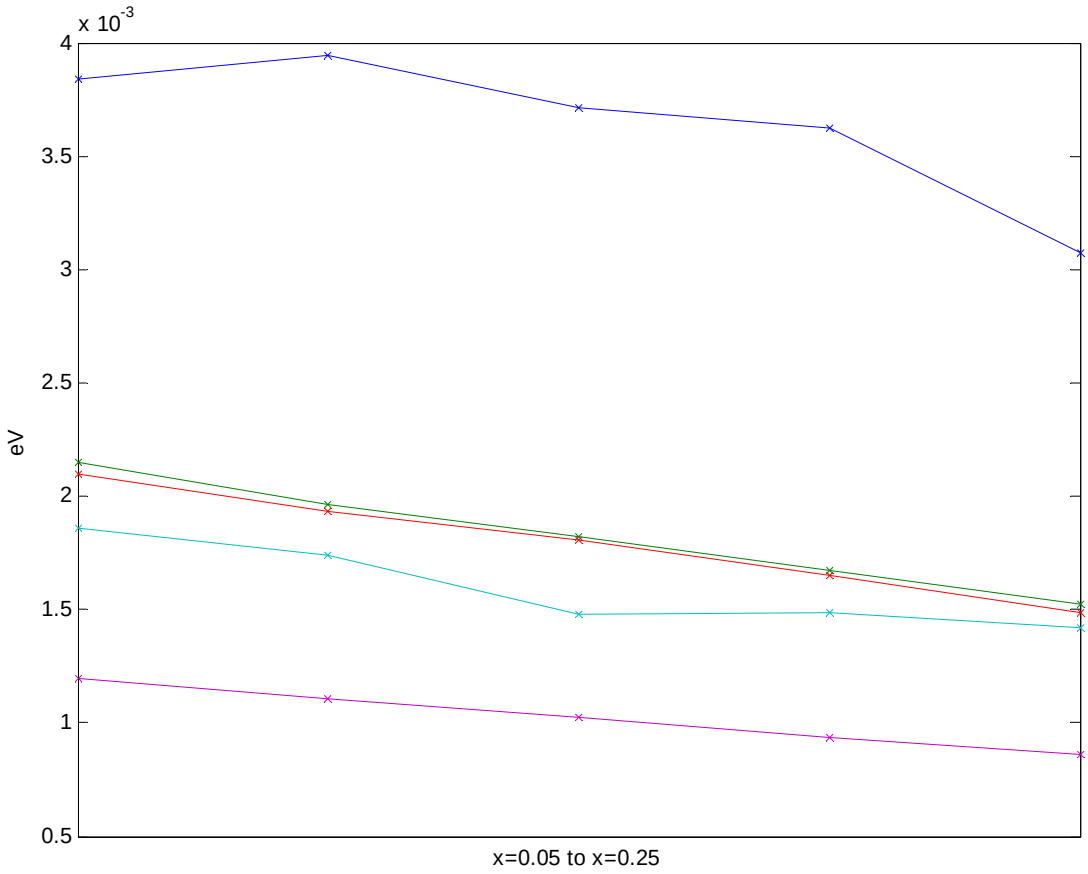

Figure3.16 the bound state energy subtract band edge energy for light hole band from ground state to 4^{th} excited state, x=0.05, x=0.1, x=0.15, x=0.2, x=0.25 totally 5 points. At x=0, heavy hole band and light hole band still degeneracy, those states are higher excited states of Γ_8^+.

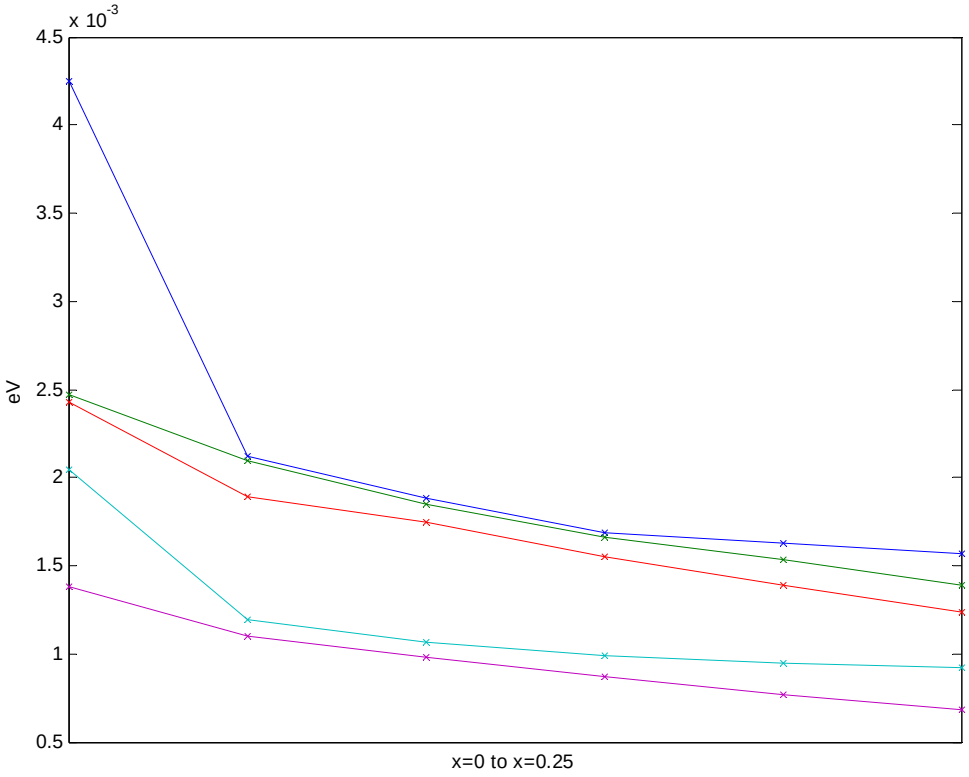

Figure3.17 the bound state energy subtract band edge energy for split of hole band from ground state to 4th excited state, x=0, x=0.05, x=0.1, x=0.15, x=0.2, x=0.25 totally 6 points.

3.3 Result

Comparing with the result of Buczkor and Bassani, the calculated energy of resonant states at unstrained case (x=0) can be fitted very well at table 3.1 and table 3.2.

Comparing with other experiments at table 3.3, our calculations are similar for the experiments data. But all the experiment data only for the case of bulk Si (x=0). No experiment reference data for the energy of strained $Si_{1-x}Ge_x$ compound is found for the further comparison. From the comparison result, our theorem calculation can be used on both strained and unstrained $Si_{1-x}Ge_x$/Si materials.

In the Γ_8^+ case of Table3.3, the result for our works and the reference of ground state and first two excited states are very close. Γ_8^-, Γ_7^-, and Γ_6^- are fitted to the experiment data of higher one. The only reference of Γ_7^+ are the result to measure the Raman scattering spectrum of donor and acceptor [3]. Our calculation result is 19meV, a little lower compare to the 23meV of the reference. This result is the part which does not fit very well. We can not explain it now.

Table3.1 resonant states of even parity

	Buczko & Bassani	my work
Γ_7^+	4.39	4.25
Γ_8^+	2.60	2.47
Γ_8^+	2.56	2.43
Γ_6^+	2.54	2.41
Γ_7^+	1.90	2.04
Γ_8^+	1.44	1.38
Γ_8^+	1.41	1.36
Γ_6^+	1.40	1.33
Γ_7^+	1.20	1.19

In table3.1 the numbers are the energy from the state to the band edge of split of hole band. The Unit is meV.

Table3.2 resonant states of odd parity

	Buczko & Bassani	my work
Γ_6^-	5.34	5.64
Γ_8^-	5.26	5.42
Γ_6^-	2.41	2.41
Γ_8^-	2.35	2.34
$2\Gamma_8^- + 2\Gamma_7^- + \Gamma_6^-$	1.48 ± 0.01	1.42

In table3.2 the numbers are the energy from the state to the band edge of split of hole band. The Unit is meV.

Table3.3 Comparing with experiment data of energy states above heavy hole band. The Unit is meV.

	Solid State Comm. 33 277 (1979)	Solid State Comm. 23 733 (1977)	PRB 27 4826 (1983)	PR 163 686 (1967)	PRL 18 608 (1967)	J. Appl. Phys. 52 5148 (1981)	Rep. Prog. Phys. 44 1297 (1981)	Solid State Comm. 15 1403 (1974)	our work
Γ_8^+ ground state	45.83	45.25±0.25	44.39	44.32		44.3	45.71	43.71	44.6
Γ_8^+	13.44±0.1	12.86±0.1							13.01
	6.38±0.1	5.8±0.1							6.66
	3.85±0.15	3.27±0.15							5.89
	2.7±0.2	2.12±0.2							3.68
Γ_8^-	14.83±0.1	14.02	13.94		13.93	15.33			15.75
	10.71±0.1	9.9	9.79		9.71	11.18	9.19		11.24
		6.04	5.97		5.86	7.36	5.34		6.58
		4.48	4.41			6.03	3.8		4.99
		3.48	2.8			4.19	2.26		3.59
		2.33	1.82			3.52	1.55		
Γ_7^-			4.8	4.68		4.25	6.1	4.11	6.05
Γ_6^-			4.72	4.41			5.79	4.03	5.18
			2.48	1.82			3.52	1.55	2.36
Γ_7^+					23				19.0

Ref. [3] ~ Ref. [9]

IV. Conclusion

The studies use projection operator, to effectively choose the acceptor wave functions for the case $Si_{1-x}Ge_x$/Si structure included stress with spin-orbital interaction considered. Then select the true resonant states, to determine the B-doped acceptor states energy.

The calculation result can fit into those experiment data in other research closely. Consequently, the calculation results of strained B-doped $Si_{1-x}Ge_x$ are credible. This model can be used to other acceptor states energy problems for strained semiconductor material. Just need to change the material parameter.

In the future study, the decision of resonant states can use Green function to determine the live time of the states and other characteristics.

Appendix I

There are 32 kinds of crystallographic point groups in nature. Each one has corresponding character table, symmetry operators, irreducible representation, and the corresponding bases of each irreducible representation.

The numbers in character table are characters. First row is the irreducible representation. $\Gamma_1 \sim \Gamma_5$ are single-valued representations. Γ_6 and Γ_7 are double-valued representations.

First column is the symmetry operators of D_{2d} group:

E: identity.

C_z: rotate 180 degree by z axis.

C_x: rotate 180 degree by x axis.

C_y: rotate 180 degree by y axis.

S_4: rotate 90 degree by z axis clockwise, then doing space inversion.

σ_d: refection by diagonal plane.

R: rotate 360 degree by z axis.

RP: operation of P first, then rotate 360 degree by z axis.

The difference of single-valued representations and double-valued representations are the value of P and RP. The value of P and RP are the same for single-valued representations. It is different for double-valued representations.

Appendix 1.1 The character table of D_{2d} group

D_{2d}	$1E$	$1R$	C_z, RC_z	(C_x, C_y) $R(C_x, C_y)$	$2S_4$	$2RS_4$	$2\sigma_d, 2R\sigma_d$
Γ_1	1	1	1	1	1	1	1
Γ_2	1	1	1	−1	1	1	−1
Γ_3	1	1	1	1	−1	−1	−1
Γ_4	1	1	1	−1	−1	−1	1
Γ_5	2	2	−2	0	0	0	0
Γ_6	2	−2	0	0	$\sqrt{2}$	$-\sqrt{2}$	0
Γ_7	2	−2	0	0	$-\sqrt{2}$	$\sqrt{2}$	0

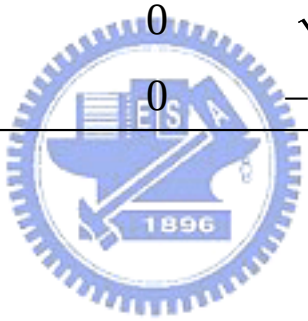

Reference

[1] S. Zwerdling, K. J. Button, B. Lax, and L. M. Roth, "Internal impurity levels in semiconductors:experiments in p-type silicon" Phys. Rev. Lett. **4**, 173 (1960)

[2] A. Onton, P. Fisher, and A. K. Ramdas, "Spectroscopic investigation of grop-III acceptor states in silicon" Phys. Rev. **163**, 686 (1967)

[3] G. B. Wright and A. Mooradian, "Raman scattering from donor and acceptor impurities in silicon" Phys. Rev. Letters **18**, 608 (1967)

[4] M. L. W. Thewalt, "Even-parity acceptr excited states in Si from bound exciton two hole transitions" Solid State Comm. **23**, 733 (1973)

[5] K. Niizeki and M. Endo, "CPA conductivity of a binary alloy with off-diagonal disorder" Solid State Comm. **14**, 687 (1974)

[6] M. S. Skolmick, L. Eaves, R. A. Stradling and J. C. Portal, S. Askenazy, "Far infrared photoconductivity from majority and minority impurities in high purity Si and Ge" Solid State Comm. **15**, 1403 (1974)

[7] A K Ramdas and S Rodriguez, "Spectroscopy of the solid-state analogues of the hydrogen atom:donors and acceptors in semiconductors" Rep. Prog. Phys. **44**, 1297 (1981)

[8] Colin E. Jones, David Schafer, Walter Scott, and R. J. Hager, "Carbon-acceptor pair centers (X centers) in silicon" J. Appl. Phys. **52**, 5148 (1981)

[9] David W. Fischer and John J. Rome, "Additional structure in infrared excitation spectra of group-III acceptors in silicon"

Phys.Rev.B **27**,4826 (1983)

[10] I.V.Altukhov, E.G.Chirkova, V.P.Sinis, and M.S.Kagan, "Towards Si1-xGex quantum-well resonant-state terahertz laser " Phys.Lett. **79**,3909 (2001)

[11] D.Schechter, "Theory of shallow acceptor resonant state in Si and Ge" J.Phys.Chem.Solids. **23**,237 (1961)

[12] N.O.Lipari, A.Baldereschi, and M.L.W.Thewalt, "Central cell effects on acceptor spectra in Si and Ge" Solid State Comm. **33**,277 (1980)

[13] J.M.Lutting and W.Kohn, "Motion of electrons and holes in perturbed periodic fields" Phys.Rev. **97**,869 (1955)

[14] R.Buczko and F.Bassani, "Shallow acceptor resonant states in Si and Ge" Phys.Rev.B **45**,5838 (1992)

[15] U.Fano, "Effects of configuration on intensities and phase shifts" Phys.Rev. **124**,1866 (1961)

[16] S.L.Chuang,Physics of Optoelectronics Devices Wiley, 1995, p147-149

[17] Martin M.Rieger and P.Vogl, "Electronic-band parameters in strained Si1-xGex alloys on Si1-yGey substrates" Phys.Rev.B **48**,14276 (1993)